PROCEEDINGS : CAMME–1996
©NML JAMSHEDPUR; pp.130-140

Mathematical modelling of austempering by finite element method

A. ROY, N. DHANG*, O.P. GUPTA**, I. MANNA***

CEBU, TELCO, Jamshedpur
**Dept. of Civil Engineering, I.I.T., Kharagpur*
***Dept. of Mechanical Engineering, I.I.T., Kharagpur*
****Dept. of Metallurgical & Materials Engineering, I.I.T., Kharagpur*

ABSTRACT

Austempered ductile iron (ADI) possesses a superior toughness than ordinary cast iron because the residual phase associated with bainitic ferrite is retained austenite instead of martensite or carbide. The desired microstructure (devoid of pearlite, martensite or carbide) can be obtained provided the effective cooling rates at different cross-sections are accurately determinable for components with varying shape, composition and heat treatment requirements. In this study, a finite element model (FEM) has been developed to predict the temperature profile along different cross-sections following austenitizing at 870°C and austempering at 370°C. Solid bodies of different shapes have been meshed into hexahedron elements by the present software. The overall global matrix equation has been numerically solved by the Gaussian elimination method. Finally, it is found that the results predicted by the present model is in well accordance with the relevant experimental data on austemperability.

NOMENCLATURE

ρ = density
K = conductivity
H = coefficient of convection
C_p = specific heat at constant pressure
T_x = temperature at a distance x
T_o = temperature of the medium
T_I = initial temperature of the body

ξ,η,ζ = local coordinates along the x, y and z directions
$\bar{n}$ = normal vector to the surface
υ = coefficient of kinematic viscosity
β = coefficient of linear expansion

INTRODUCTION

Spheroidal graphitic (SG) cast iron with a bainitic microstructure is called austempered ductile iron (ADI). The high Si content of ADI significantly inhibits the onset of carbide precipitation during the austenite to bainite transformation at 370°C or above[1]. The residual phase present within the bainitic sheaves are high-C stabilized retained austenite[2]. The unique combination of high tensile strength (700–1600 MPa UTS[3]), moderate ductility (3.8–16% elongation[3]), superior toughness (35-100 J[3]) and high contact fatigue strength (ΔK_{th} = 3.2–7.8 MPa$\sqrt{m}$[4]) of the ADI components is mainly attributed to the presence of the aforesaid thermally and mechanically stable retained austenite. In addition, the favorable physical properties of cast irons (lower density, superior damping property and thermal conductivity) as compared to those of steel, and the scope of drastic reduction in machining costs (in the case of near net shape castings) are the reasons behind the increasing use of ADI as raw materials for manufacturing crank shafts and tooth points in automobile and excavator industries. Recently, Indian automobile industries like TELCO have shown a great interest in using ADI for critical automobile and excavator parts. However, a relatively higher Mn-content and its associated danger of Mn-segregation in the interdendritic and intercellular areas of the as-cast irons in the automobile industries. Mn-segregation either leads to incomplete transformation of austenite to bainite or precipitation of carbide to reduce the toughness of the product. In this regard, a well-orchestrated research attention is warranted to develop suitable grades of cast iron, and more so, device-appropriate heat treatment schedules to utilize ADI for automobile and earthmover components.

Accurate prediction of austemperability is, therefore, necessary to determine the precise amount of alloying additions required for a particular application. The experimental results available in the literature are applicable only for simple component geometry (say, cylindrical rod)[5]. Extrapolation of these observations to the actual complex components like gears, crank shafts, *etc.* requires rigorous mathematical treatment taking into considerations all the complexities which may be

present during any industrial heat treatment. This is now feasible by adopting an advanced numerical technique like finite element method (FEM), boundary element method (BEM) and finite difference method (FDM), and utilizing a high speed main frame computer.

In the present paper, an attempt has been made to generate the thermal profile of a cast iron component during the quenching from austenitizing to austempening temperature (Fig. 1). The material used here is unalloyed SG iron. The dimension of the job considered is 1 cm^3, as it has earlier been predicted[5] that an unalloyed ADI component may be fully austempered at 370°C for a rod of 1 cm diameter (Fig. 2). Finally, the present model and its predicted results have been validated by a suitable comparison with the relevant experimental data.

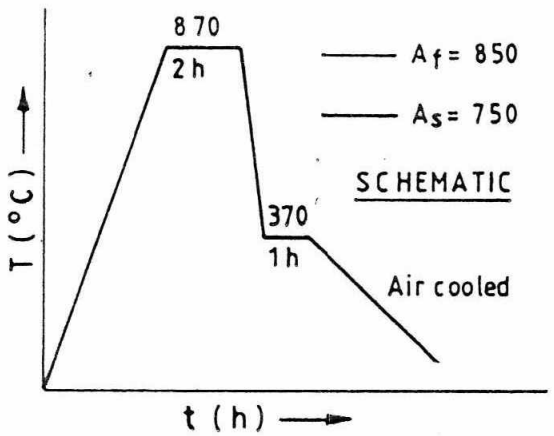

Fig. 1 : Typical heat treatment schedule for producing upper bainitic microstructure

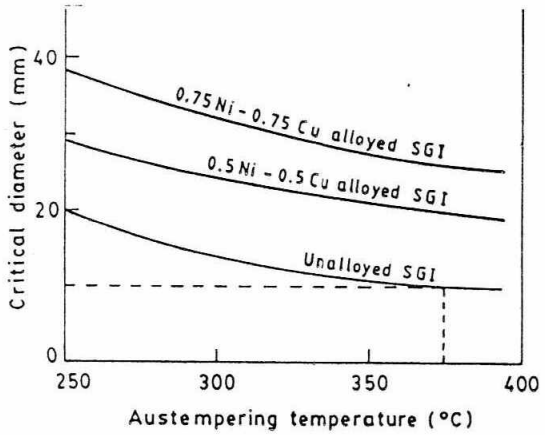

Fig. 2 : Variation of component size with austempering temperature for different grades of cast iron (after [15])

FORMULATION OF THE PROBLEM

The body under present investigations was quenched into an austempering bath (Fig. 3) from 870°C. It was assumed that there was no heat loss during the possible delay in quenching. The coefficient of convection was calculated (Appendix I) considering the bath composition as $NaNO_2$ (40%) + KNO_3 (53%) + $NaNO_3$ (7%) with a melting point of 148°C. The bath volume is infinite and eliminates a possible temperature rise after quenching. A Jominy end quench test was carried out to determine the critical cooling rate of the present material (Fig. 4). At a distance of 5.2 mm from the quenched end, the observed hardness dropped to an average value of R_C50. This is reported to be equivalent to the semi-martensitic hardness of a 0.53–0.62 %C steel [6]. Assuming one dimensional heat flow along the x direction (of infinite length), the heat balance in the specimen may be expressed as:

$$\rho C_p \frac{\partial T}{\partial t} = K \frac{\partial^2 T}{\partial x^2} \qquad \ldots 1$$

A simple error function solution of equation (1) may be:

$$\frac{T_x - T_0}{T_i - T_0} = \text{erf}\left(\frac{x}{2\sqrt{ht}}\right) \text{ where } h = \frac{K}{\rho C_p} \qquad \ldots 2$$

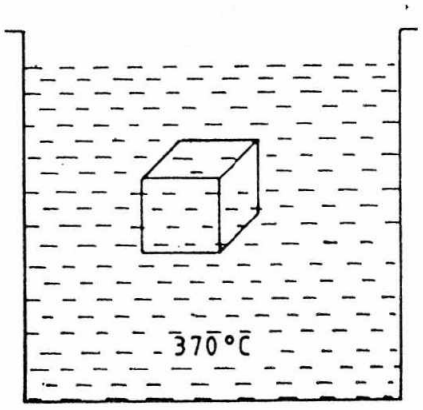

Fig. 3 : A typical austempering bath maintained at 370°C with a body undergoing the heat treatment cycle adopted in this study

Calculations show that the temperature drops from 870°C to 370°C in roughly 1.9s at x = 5.2 mm. This rate of cooling was assumed to be

the critical cooling rate of the SG iron under present investigation. A finite element analysis to solve the three dimensional heat flow condition within the austempering bath has been described in the following section. Variation of temperature with time has been computed at different nodes to compare the cooling rates across various sections with the critical cooling rate.

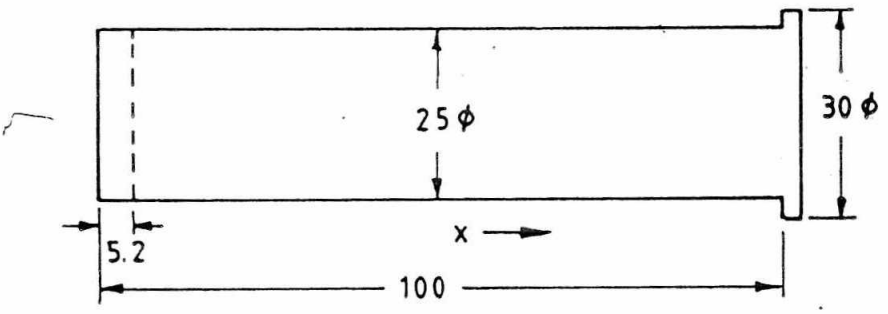

Fig. 4 : A Jominy specimen of an unalloyed SG iron showing distance from the quenched end with an average hardness of RC50

NUMERICAL ANALYSIS

The cubic geometry of the specimen was divided into 125 isoparametric hexahedral elements as shown in Fig. 5. The shape functions were defined [7] as follows :

$$\begin{bmatrix} N_1 \\ N_2 \\ N_3 \\ N_4 \\ N_5 \\ N_6 \\ N_7 \\ N_8 \end{bmatrix} = \frac{1}{8} \begin{bmatrix} (1-\xi) & (1-\eta) & (1-\zeta) \\ (1-\xi) & (1+\eta) & (1-\zeta) \\ (1+\xi) & (1+\eta) & (1-\zeta) \\ (1+\xi) & (1-\eta) & (1-\zeta) \\ (1-\xi) & (1-\eta) & (1+\zeta) \\ (1-\xi) & (1+\eta) & (1+\zeta) \\ (1+\xi) & (1+\eta) & (1+\zeta) \\ (1+\xi) & (1-\eta) & (1+\zeta) \end{bmatrix} \quad \ldots 3$$

The governing equation expressing the heat balance within the body on account of three dimensional heat conduction may be expressed as:

$$\rho C_p \frac{\partial T}{\partial t} = K \left\{ \frac{\partial^2 T}{\partial x^2} + \frac{\partial^2 T}{\partial y^2} + \frac{\partial^2 T}{\partial z^2} \right\} \quad \ldots 4$$

with the following boundary condition :

$$-K\frac{\partial T}{\partial n} = H\,(T - T_0) \qquad \ldots 5$$

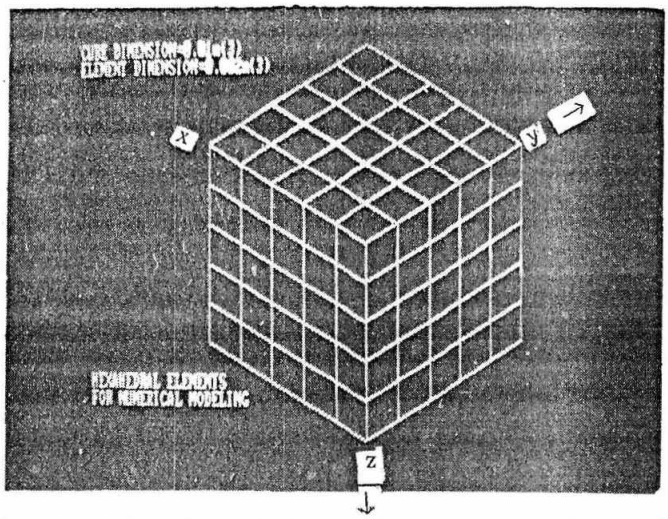

Fig. 5 : Idealized hexahedral elements for numerical modelling

The material constants were determined as per Appendix I.

Galerkin's weighted residual technique was adopted to arrive at the overall matrix equation,

$$[M]T + [\overline{K} + \overline{H}]T = [F] \qquad \ldots 6$$

where,

$$M_{ij} = \rho C_{pv}\int N_i N_j dv \qquad \ldots 7$$

$$\overline{K}_{ij} = K\int_v \left(\frac{\partial N_i}{\partial x}\frac{\partial N_j}{\partial x} + \frac{\partial N_i}{\partial y}\frac{\partial N_j}{\partial y} + \frac{\partial N_i}{\partial z}\frac{\partial N_j}{\partial z}\right) dxdydz \qquad \ldots 8$$

$$H = H_s\int N_i N_j ds \qquad \ldots 9$$

$$F = HT_{0s}\int N_i\, ds. \qquad \ldots 10$$

The time integration was computed directly assuming a linear variation of temperature within a time interval of 0.002 seconds as per Galerkin's unconditionally stable time integration scheme [8]:

$$\left(\frac{[M]}{\Delta t} + \beta\left[\overline{K} + \overline{H}\right]\right)[T_{n+1}] = \left\{\frac{[M]}{\Delta t} - (1-\beta)\left[\overline{K} + \overline{H}\right]\right\}[T]_n + [F] \qquad \ldots 11$$

for $\beta = 2/3$.

An indigenously developed software was used to carry out the mesh generations as well as the above mentioned computations. Integrations were performed numerically at various stages by using the 4-point Gauss quadrature technique [7]. The global matrix inversion for solving equation (7) was carried out using the Gaussian elimination method. Temperatures at each node, after each time step, was calculated and the temperature within an element was evaluated as per the following interpolation relations :

$$T = \sum_{i=1}^{8} N_i T_i \qquad \ldots 12$$

The total temperature range (870–370°C) was divided into fifteen equal temperature zones each of which was assigned a particular color. The temperature contours on different sections of the cube were determined after various time intervals.

RESULTS AND DISCUSSION

Temperature contours on two different sections (222) and (200) are presented in Fig. 6-13. These two sections were selected due to the following reasons: 1) From the nature of the temperature distribution across the (222) plane, thermal and transformational stresses generated on the sharp corners of the cube may be computed. Consequently, the amount of distortion of the component due to austempering may be ascertained prior to treatments of expensive semifinished components. Moreover, the integrity of the analysis may be verified by observing differences in the cooling rates generated between the face and the edge.

It is evident from Fig. 6 that some areas along the face of the job were at a higher temperature than areas adjacent to the edge upto a certain distance inside the body. This is an interesting prediction of the model which may not be observed in practice as the time elapsed is only 0.02 seconds. The central high temperature zone is symmetrically elongated in the direction of the faces and the low temperature zone is extended along the edges. Fig. 7 illustrates that the plane is bounded by a low temperature zone in addition to the trends observed in Fig. 6. After 1.4 seconds (Fig. 8), the central portion of the section had cooled below 600°C. Figs. 9-10 evidences the extension of the low tempera-

ture frcm boundary towards the center. After 1.7 seconds from the start of the quenching (Fig. 11), the whole section has cooled down below 370°C, and thereby, satisfies the predefined condition of suppression of pearlite formation.

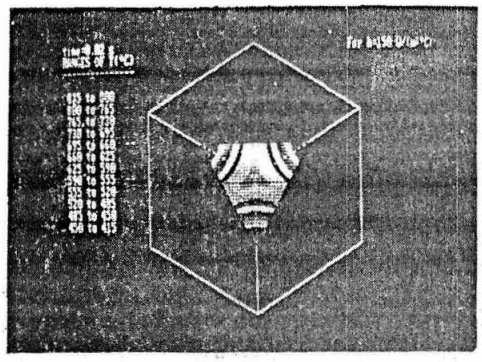

Fig. 6 : Temperature contours on the (222) section at 0.02 seconds after quenching to 370°C

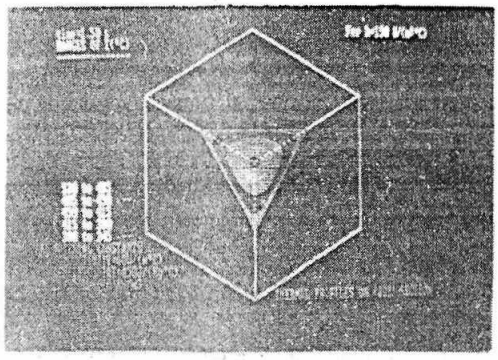

Fig. 7 : Temperature contours on the (222) section at 1.2 seconds after quenching to 370°C

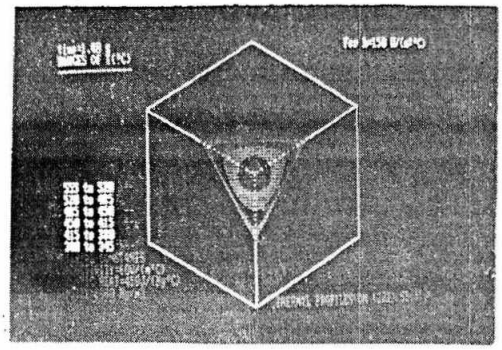

Fig.8: Temperature contours on the (222) section at 1.4 seconds after quenching to 370°C

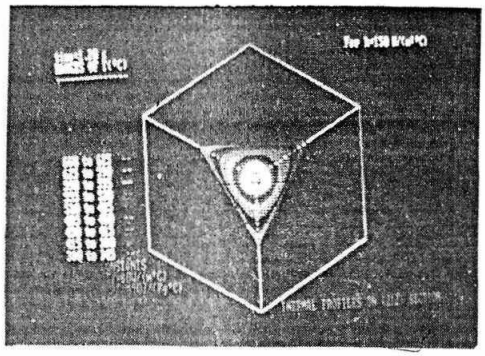

Fig.9:Temperature contours on the (222) section at 1.5 seconds after quenching to 370°C

Cooling rates at the core of (200) section is expected to be minimum as it represents the central layer of the body. Therefore, if the cooling rate at the concerned region is greater than the critical cooling rate, pearlite formation may be suppressed in the body. Figs. 12-13 illustrates that the entire (200) section has reached 370°C after an elapsed time of 1.7 seconds. Therefore, the prediction of the present

model show reasonable agreement with experimental observations. However, it was also observed that the time temperature plots at the center of the observed sections exhibited a sigmoidal profile instead of the expected exponential decay. The fact that thecoefficient of convection was assumed constant during the quenching may give rise to this discrepancy. In actual industrial situation the temperature of the bath may rise by 10–15°C immediately after quenching. As a result, the value of the coefficient of convection may vary significantly, and consequently, the actual temperature time plots may deviate from the predicted nature.

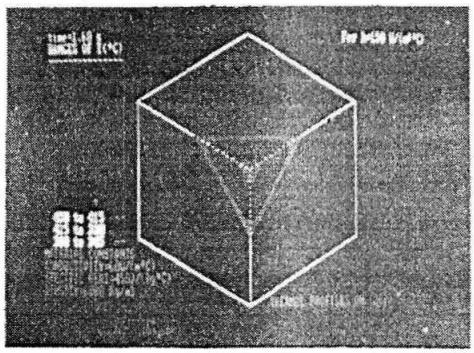

Fig.10:Temperature contours on the (222) section at 1.6 seconds after quenching to 370°C

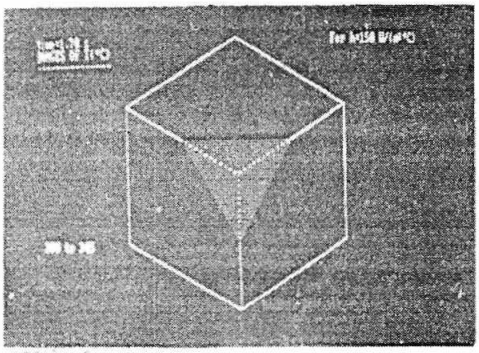

Fig.11:Temperature contours on the (222) section at 1.7 seconds after quenching to 370°C

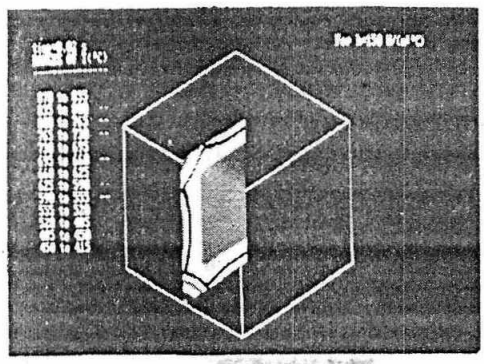

Fig.12 : Temperature contours on the (222) section at 0.02 seconds after quenching to 370°C

CONCLUSIONS

A novel numerical approach based on three dimensional finite element has been presented for the prediction of austemperability of SG iron. The present model allows both accurate simulation of the thermal profile within the job and the heat flow conditions existing in the austempering bath. The computed three dimensional temperature profile and its associated microstructure reveal excellent agreement with the relevant experimental data on austempering. Several complex features associated with the cooling patterns of different parts of the body have been identified. The effect of these on austemperability has not been reported in the relevant literature. It has been found that the stress generated on the corner points may not be significant. On the other hand, factors like nodule count and component geometry may remarkably influence the cooling rates. Finally, further modifications are being incorporated in our model in the next phase of development to take the temperature dependence of the heat transfer coefficients and enthalpy changes due to concomitant phase transitions within the material into account.

ACKNOWLEDGMENT

The authors are grateful to TELCO, Jamshedpur for extending support for the present investigation.

REFERENCES

[1] S.J. Matas and R.F. Hehemann, "Structure of bainite in hypoeutectoid steels", *AIME Trans.*, Vol. 221, 1961, pp179-185.

[2] H.K. Bhadeshia, and J.W. Christian, "Bainite in steels", *Metallurgical Transactions, A*, Vol. 21A, 1990, pp767-797.

[3] R. Elliot, *"Cast Iron Technology"*, Butterworth Publications, London, UK, pp141.

[4] I. Singh and S.K. Putatunda, *IIM Trans.*, Vol. 47, 1994, pp317-325.

[5] N. Darwish and R. Elliot, "Austempering of low-Mn ductile irons", *Mater. Sc. Tech.*", Vol. 9, 1993, pp572-585.

[6] H.H. Hobhkob, *"Theory of Heat Treatment of Metals"*, pp284.

[7] W.D. Pepper and J.C. Heinrich, *"Finite Element Method Basic Concepts and Applications"*, pp160-180.

[8] R.D. Cook, D.S. Malkus and E.M. Plesha, *"Concepts and Applications of Finite Element Analysis"*, 1973, pp485.

[9] Kozlovsky, *"Handbook of Heat Transfer"*, Mashinstroenie Publishers, Moscow, 1967, pp106-285.

APPENDIX I

Calculation of coefficient of convection for the saltpeter mixture

Heat transfer takes place from/to a body located in unlimited space due to free convection satisfying the relation:

$$N_u = C\,(P_r G_r)^n$$

where, N_u = Nusselt number, P_r = Prandtl number, G_r = Grashof number and C, n are constants.

P_r for saltpeter mixture at 370°C = 8.52[9]. G_r may be expressed as:

$$G_r = \frac{gl^3\beta\Delta T}{\upsilon^2}$$

β was calculated to be 4.33 x 10^{-5}/°C using the formula $\rho_{150}=\rho_{370}(1+\beta\Delta T)$ and υ = 1.158536 x 10^{-6} m^2/s. ΔT was approximated to be unity. Therefore, $G_r P_r$ = 3983.4019 and hence, C = 0.54 and n = 1/4[9].

From the relation N_u = H1/K, the value of H was found ≈ 150 $W/m^2/°C$.

Values of other parameters utilized for the calculations are :

C_p for cast iron = 450 J/Kg/°C [9]

ρ = 6080 kg/m^3 [9].